Desalination and Water Treatment
www.deswater.com
doi: 10.5004/dwt.2021.27889

243 (2021) 275–286
December

Regeneration of anthraquinone dye-loaded waste activated carbon by microwave heating and its reuse to adsorb dye-containing wastewater

Chunfu Xin[a,b,c,d], Wenhai Hu[a,b,c,d], Hongying Xia[a,b,c,d,*], Qi Zhang[a,b,c,d], Heng Yan[a,b,c,d]

[a]*State Key Laboratory of Complex Nonferrous Metal Resources Clean Utilization, Kunming University of Science and Technology, Kunming 650093, Yunnan, China, emails: hyxiakust@163.com (H. Xia), xin1057781417@163.com (C. Xin), 1783240500@qq.com (W. Hu), 1396835730@qq.com (Q. Zhang), 857384078@qq.com (H. Yan)*
[b]*Yunnan Provincial Key Laboratory of Intensification Metallurgy, Kunming University of Science and Technology, Kunming 650093, Yunnan, China*
[c]*Key Laboratory of Unconventional Metallurgy, Ministry of Education, Kunming 650093, Yunnan, China*
[d]*Faculty of Metallurgy and Energy Engineering, Kunming University of Science and Technology, Kunming 650093, Yunnan, China*

Received 19 May 2021; Accepted 1 October 2021

ABSTRACT

This study investigated the regeneration of waste activated carbon (AC) that contains anthraquinone dye, by microwave irradiation. The adsorption isotherm and adsorption kinetics were analyzed by batch adsorption experiments in which Methylene blue (MB) dye and Malachite green (MG) dye were chosen as the adsorbates. The effects of microwave heating power, heating temperature and holding time on the adsorption capacity of regenerated AC were investigated. The Brunauer–Emmett–Teller equation, scanning electron microscopy, X-ray photoelectron spectroscopy and Raman spectra were used to characterize spent waste AC and regenerated AC. The results showed that microwave heating efficiently preserved the porous structure of the regenerated AC to restore the original activation sites and adsorption capacity. The specific surface area of regenerated AC was 634.73 m^2/g, the maximum adsorption capacities of MB and MG were 265.65 and 366.89 mg/g, respectively, and the C–O functional groups on the surface of AC increased significantly. The adsorption isotherm was confirmed by the Langmuir isotherm, and the adsorption process could be accurately described by the pseudo-second-order kinetic model. In addition, the power consumption of microwave regeneration was significantly lower than that of traditional regeneration methods, which represented a significant improvement in adsorption chemistry.

Keywords: Waste activated carbon; Microwave heating; Anthraquinone dye; Regeneration; Adsorption

1. Introduction

Concerning about sustainable development and environmental protection, pollution and waste from industrial production are increasing. Wastewater with a high color degree from print and dye is considered the most harmful contaminant in the textile industry [1,2]. Anthraquinone, one of the most permanent dyes with stable properties, can resist solar radiation and harsh environmental conditions; thus, it is difficult to degrade anthraquinone. Anthraquinone dye must be removed from printing and dyeing wastewater because of its "toxicity" [3,4]. Ecologically, the human eye can detect a concentration of 0.005 mg/L reactive dye in water [5]. Therefore, the dye concentration in printing and dying water must be reduced as low as possible. The most effective method of dye wastewater decoloration seems to be photocatalytic degradation or photochemical oxidation, followed by removal of organics or another by-product

* Corresponding author.

by biological methods [6,7]. For anthraquinone dye, these degradation and oxidation methods are difficult to work because of its stable properties [8]. It is necessary to introduce new, more efficient oxidants or a new method to treat wastewater containing anthraquinone dye [9].

Adsorption methods have been proven successful in decoloring textile effluents, and they are an effective method to treat wastewater containing anthraquinone dyes [10,11]. However, this treatment method is limited by the high cost of adsorbents such as activated carbon (AC). Although powder AC and low-cost adsorbents can be disposed of directly, wastewater sludge and spent adsorbents are regarded as hazardous solid waste, and direct disposal is forbidden by law in some countries [12]. In industry, granular activated material is usually put into cylindrical objects to adsorb contaminants from wastewater passing through it. The packed columns were used until the AC was filled with contaminants and lost its adsorption capacity. Once AC saturation adsorption occurs, the columns must be replaced to restore its adsorption capacity [13]. Generation as a typical method is more economical than replacement [14]. AC is a rough form of graphite with a high specific surface area, amorphous pore structures, and a variety of pore sizes. Formerly, waste AC is usually discarded or dumped in landfills [15,16]. However, burying harmful waste carbon still pollutes the environment. Regeneration of waste AC has motivated the development of regeneration systems to permit a wider application of carbon adsorption processes and ensure their economic feasibility [17].

The traditional regeneration method of waste AC is thermal treatment, but in some situations, the thermal treatment process may take a long time, involving high energy consumption; and generating an inadequate heating rate [18]. In recent years, microwave radiation has been considered a potentially effective orientation for regeneration due to its penetrative and selective heating ability [19]. Microwave-assisted regeneration offers advantages compared with the conventional method, including rapid and accurate temperature control, energy conservation and smaller space requirements [20,21]. Microwave radiation is considered to be an efficient and feasible regeneration tool due to its ability to uniformly and instantaneously heat [22]. Compared with traditional treatment methods, microwave-assisted regeneration technology can achieve accurate temperature control, high efficiency in intermittent use, small space requirements and energy savings [19]. According to Malik et al. [23], compared with conventional heating, microwave radiation regenerates AC with high efficiency and low energy consumption. Gagliano et al. [24] also reported that AC still has adsorption capacity toward dye after regeneration, to achieve the purpose of recycling AC.

In this paper, the regeneration effect of AC assisted by microwaves was studied. The utility of microwaves for regenerating waste AC containing anthraquinone dye was explored. This representation includes nitrogen adsorption, scanning electron microscopy (SEM), Raman spectra, and X-ray photoelectron energy spectrum analysis. The original sample and regenerated samples were analyzed for their specific surface area, pore size and pore volume. The adsorption performance of the regenerated AC on dye pollutants was investigated using an initial concentration of 400 mg/L Malachite green (MG) and Methylene blue (MB) as the paradigms. The adsorption experiment results showed that the maximum adsorption amounts of regenerated AC were 265.65 mg/g for MB and 366.89 mg/g for MG under the conditions we examined. The maximum adsorption capacity of MB was higher than the values of 185 mg/g reported by Roosta et al. [25]; and 204 mg/g reported by Wabaidur et al. [26]. The maximum adsorption capacity of MG was higher than the values of 154.2 mg/g reported by Sayğılı and Güzel [27]; and 98 mg/g reported by Ahmad and Kumar [28].

2. Experiment

2.1. Chemicals

The waste AC was obtained from the factory treating dye wastewater (Liaoning, China). MB ($C_{16}H_{18}ClN_3S{\cdot}3H_2O$), MG ($C_{23}H_{25}N_2{\cdot}Cl$) and sodium hydroxide (NaOH, ≥99%) were all analytically pure and purchased from Aladdin Reagents (China). MB and MG were chosen as the adsorbate. The water used was distilled water.

2.2. Regeneration of waste AC

Waste AC (100 g) was washed with 2 g/L sodium hydroxide solution to remove impurities. The waste AC was mixed with sodium hydroxide solution in a conical flask and then placed in a thermostat steam bath vibrator (TJ ZD-85) to vibrate at 25°C and 264 rpm for 24 h. The sample was then separated and washed with distilled water under ultrasound for 3 h until it was free of sodium hydroxide. At this stage, approximately 32.5% of anthraquinone dye and other organics were eliminated due to the cavitation effect of ultrasound. Then, the sample was placed into an electrothermal blowing dry oven at 80°C for 10 h. The dried sample was put into a microwave oven, the power was set to 960 W with different heating temperatures and times, and then the sample was cooled to room temperature. The treated AC was washed to remove ash, dried and prepared for adsorption studies.

2.3. Characterization of regenerated AC

The material composition was determined by X-ray photoelectron spectroscopy (XPS). The molecular structure was characterized by Raman spectra. The pore structure properties were determined by a nitrogen adsorption–desorption apparatus at 77 K (Quantachrome, Autosorb-1-C). The specific surface area (S_{BET}) was determined by the Brunauer–Emmett–Teller equation (BET). The micropore volume (V_{mic}), micropore surface area (S_{mic}), and surface area (S_{ext}) of all materials were estimated by the *t*-plot method. The total pore volume (V_{tot}) was defined as the maximum amount of nitrogen adsorbed at a relative pressure of P/P_0 = 0.99. The average pore diameter (Dv) was calculated by the ratio $4V_T/S_{BET}$, and the pore size distribution was determined using density functional theory. SEM images were obtained using a field-emission scanning electron microscope (SEM; Philips XL30 ESEM-TMP). A box-type microwave oven was designed and manufactured by the Key Laboratory

of Unconventional Metallurgy at Kunming University of Science and Technology [29].

2.4. Adsorption experiments of regenerated AC

Batch adsorption experiments were carried out in a 250 mL Erlenmeyer flask containing 0.2 g of adsorbent (regenerated AC) and 200 mL of dye solutions with a concentration of 400 mg/L. The flasks were vibrated in a thermostat steam bath vibrator at 25°C and a shaking speed of 240 rpm for 2 h, taking samples every 10 min. The concentrations of MB and MG were determined using a double beam UV spectrophotometer (Shimadzu, Japan/UV-2600) at 668 and 618 nm, respectively. Dye solutions uptake at equilibrium, q_e (mg/g), was determined by:

$$q_e = \frac{\left(C_0 - C_e\right)V}{W} \tag{1}$$

where C_0 and C_e are liquid-phase concentrations of the dye solution at initial and equilibrium, respectively. V (L) is the volume of the dye solution, and W (g) is the mass of absorbent. Every solution sample was filtered through filter papers before test absorbance in order to reduce the interference from carbon fines.

2.5. Isotherm modeling

The equilibrium data were modeled by using Langmuir [30] Freundlich and Temkin isotherm models [31].

Langmuir isotherm:

$$q_e = \frac{Q_0 K_L C_e}{\left(1 + K_L C_e\right)} \tag{2}$$

where Q_0 (mg/g) is the adsorption constant related to adsorption capacity, and K_L (L/g) is the Langmuir constant related to adsorption energy.

Freundlich isotherm:

$$q_e = K_F C_e^{1/n} \tag{3}$$

where K_F (mg/g)(L/mg)$^{1/n}$ and $1/n$ are Freundlich adsorption constant and a measure of adsorption intensity respectively.

Temkin isotherm:

$$q_e = B\ln\left(AC_e\right) \tag{4}$$

where $B = RT/b$ which b (J/mol) is the Temkin constant related to the heat of sorption, A (L/g) is equilibrium binding constant, and R (8.314 J/mol), T (K) are gas constant and absolute temperature, respectively.

2.6. Kinetic modeling

The kinetics were investigated for the sorption of MB and MG onto regeneration AC, which is represented in Fig. 7.

The kinetic equation for pseudo-first-order kinetic Eq. (5) and pseudo-second-order kinetic Eq. (6) are as follows:

$$\log\left(q_e - q_t\right) = \log\left(q_e\right) - \frac{k_1}{2.303}t \tag{5}$$

$$\frac{t}{q_t} = \frac{1}{k_2 q_e^2} + \frac{1}{q_e} \tag{6}$$

where q_t is the amount of dye sorbed at time t (mg/g), q_e is the equilibrium capacity of the sorbent (mg/g), k_1 is the rate constant (min^{-1}), and t is the contact time (min), k_2 is the rate constant (g/mg min).

3. Results and discussion

3.1. Effect of heating temperature and time on regenerated AC

The effect of heating temperature on the specific surface area of regenerated AC is shown in Fig. 1a. The reason is that anthraquinone dye and other organic matter thermally degrade to micromolecules or gases with increasing temperature. When the temperature was raised to 900°C, the pores of AC collapsed, and the AC lost a part of the adsorption capacity [32]. The optimum temperature of the regeneration process was 800°C, and the specific surface area was 634 m^2/g.

As Fig. 1b shows, at different temperatures, the specific surface area and heating time have the same trend. With increasing heating time, the specific surface area increased and reached a maximum of 40 min. The regeneration effect was the best at 800°C held for 40 min. The decomposition of anthraquinone dye and other organic matter was not sufficient, and more than 40 min led to pore structure collapse. The conclusion was that the optimal condition was 800°C for 40 min during the regeneration process. Regenerated AC is referred to in a later section as the optimal sample that is treated at 800°C for 40 min.

3.2. Analysis of waste AC and regenerated AC

The BET isotherms are shown in Fig. 2a. A hysteretic loop existed in the isotherms of both the waste sample and the regenerated sample, which indicated that there were small mesopores in the sample. According to the International Union of Pure and Applied Chemistry (IUPAC) classification standard, the isotherm belongs to the IV type curve, and the hysteresis loop belongs to H4 [33]. The increase in the adsorption quantity after regeneration treatment indicated that the sample had more abundant pore structures [34]. Compared with the waste AC, the specific surface area of the regenerated AC increased by 521.19 m^2/g. The total pore volume increased by 0.334 mL/g, and the micropore ratio increased by 28%. The results indicated that microwave heating worked effectively, which expanded the pore volume and reduced the pore diameter. In the treatment of wastewater by regenerated AC, the dye molecules will stick to the surface of the AC [35]. Fig. 2b shows the pore size distribution of these two samples. The pore size distribution of AC can clearly show the proportion of pore volume that molecules can enter, and reflects the shape, size and morphology of the pore structure of AC [36,37]. As Fig. 2b shows, the peak value of pore size ranged from

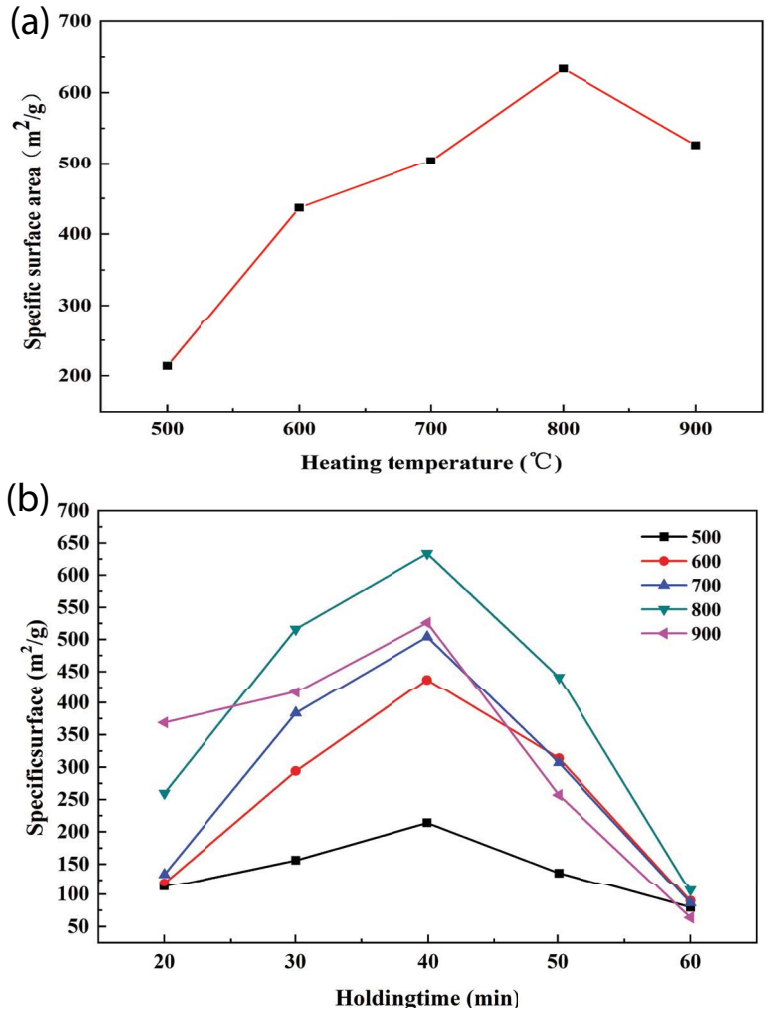

Fig. 1. (a) Effect of temperature on waste activated carbon regeneration and (b) effect of holding time on waste activated carbon regeneration.

1 to 5 nm for both samples. Compared with waste AC, the pore volume of regenerated AC was higher, which meant that waste AC formed more pore structures after microwave heating regeneration. The pore structure parameters and pore size of waste AC and regenerated AC are shown in Table 1 [38].

3.3. SEM analysis

The surface of waste activated carbon, as shown in Fig. 3a is highly packed, dense, uneven, and rough with mini pores. Many impurities adhered to the surface of waste AC, including anthraquinone dye and other contaminants. Except for some small pores, the pore structure is almost invisible on the waste activated carbon, which shows that the waste activated carbon has almost lost its adsorption capacity. Fig. 3b shows the surface pore structure of regenerated AC. A clear and abundant pore structure can be seen on the surface of the regenerated activated carbon at 30 μm. The SEM figure indicated that contaminants adhered to the pores were degraded and created new pores. There was still a small amount of attachment in the pore in Fig. 3b. This result may be residual organic pollutants in the AC after degradation. This situation did not affect the adsorption performance of regenerated AC. This shows that the waste activated carbon is heated by microwaves to remove a large amount of internal impurities, so that the regenerated activated carbon has a large number of pore structures and restores the adsorption capacity.

3.4. XPS analysis

The deconvolution of the C1s signals can identify the chemical states and environment of the carbon atoms [38]. As shown in Figs. 4a and b, the peak strength of these elements at the binding energy are 284.74, which indicates that the central element is carbon. Fig. 4a shows the spectra of waste AC, and Fig. 4b shows the spectra of regenerated AC. The peaks located at 284.68 and 286.46 eV were attributed to the functional groups C–C and C–O, respectively. The C–C functional group of regenerated AC was almost the same as that of waste AC. However, the binding energy of the C–O functional group changed from 286.46 to 286.91, and the content of C–O increased from 6.35% to 27.46%

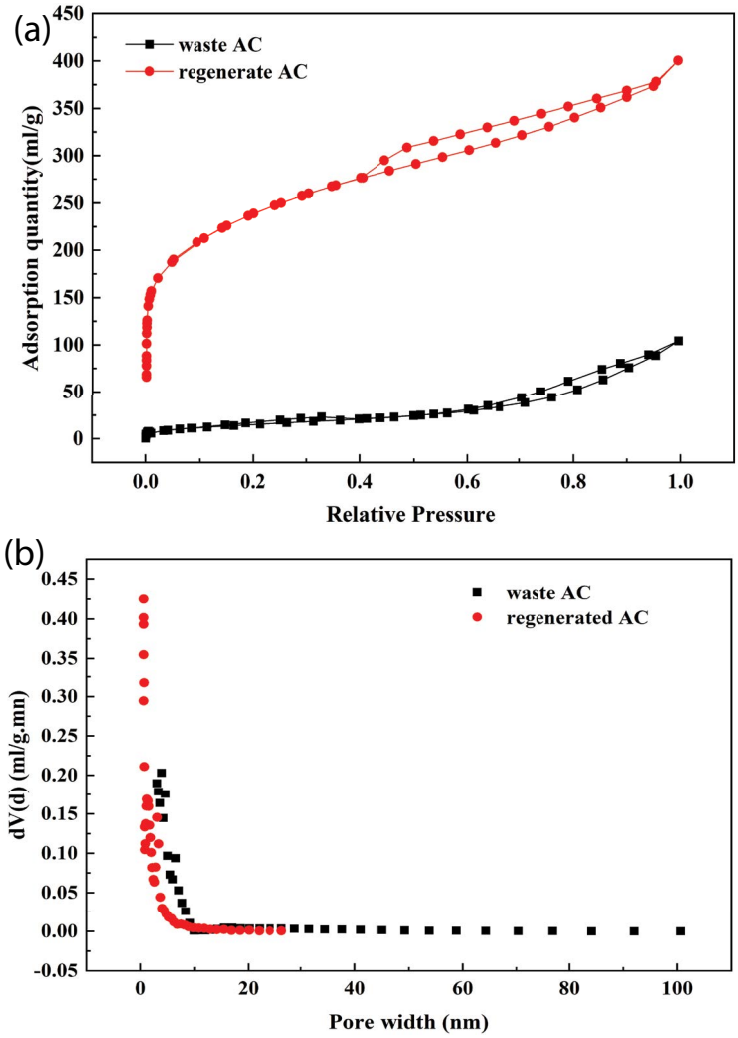

Fig. 2. (a) N_2 adsorption and desorption isotherm of waste activated carbon and regenerated activated carbon and (b) pore size distribution of waste activated carbon and regenerated activated carbon.

Table 1
Pore structure parameters of activated carbon

Item	Surface area (m^2/g)	Total pore volume (mL/g)	Average pore size (nm)	Micropore volume (mL/g)	Micropore ratio
Waste activated carbon	634.73	0.3764	2.91	0.0873	23%
Regenerated activated carbon	113.54	0.7104	2.83	0.364	51%

after regeneration. This result indicates that the binding energy of AC was changed after regeneration by microwave from the waste AC [39,40]. The increase in oxygen and carbon contents confirmed that the microwave heating regeneration process effectively modified the surface of regenerated AC [41]. Therefore, the microwave heating regeneration process can produce a larger pore volume and a richer surface chemical structure. Microwave heating leads to more oxygen-containing functional groups on the surface of AC. The formation of these functional groups is expected to play an important role in adsorption. Surface functional groups play an important role in evaluating the adsorption capacity of materials [42].

3.5. Raman analysis

The Raman spectra were introduced to understand the ordered/disordered crystal of the waste and regenerated AC, as shown in Fig. 5. Typical bands of these two samples are both at approximately 1,350 (D band) and 1,600 cm^{-1} (G band). The degree of carbonization of both samples could be described by the value of R (I_D/I_G). The R-value of

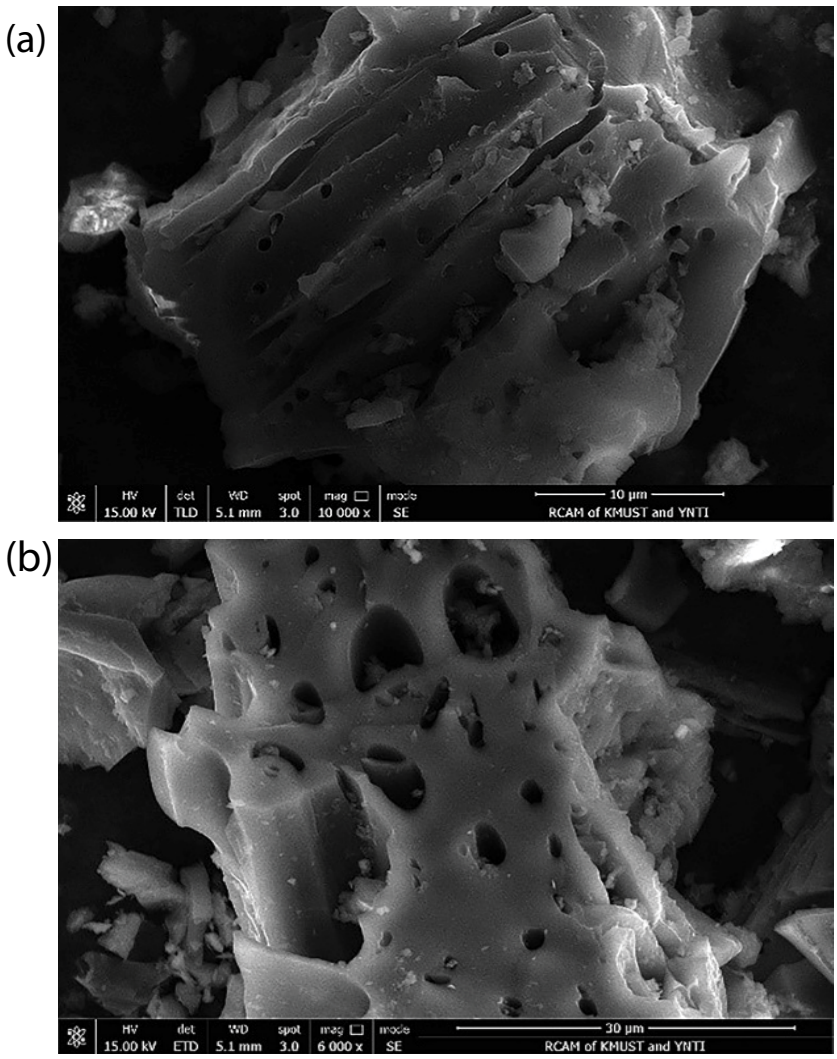

Fig. 3. (a) Waste activated carbon and (b) regenerated activated carbon.

regenerated AC (I_D/I_G = 1.037) was larger than the *R*-value of waste AC (I_D/I_G = 0.887). The results show that the graphite microcrystalline structure of the regenerated AC is destroyed, indicating that there are many unsaturated carbon atoms on its surface, which proves that more functional groups are produced after microwave heating. The Raman spectra were consistent with the XPS spectra analysis [43].

3.6. Adsorption isotherms analysis

The adsorption isotherm was used to describe the relationship between adsorbent molecules and the adsorbent surface. The adsorption mechanism and rule of the adsorbent can be described by the adsorption isotherm analysis in the process of adsorption, which were fitted by the Langmuir, Freundlich and Temkin isothermal equations [44]. Table 2 shows the data of the experiment in which MB and MG solutions were adsorbed by regenerated AC at 303 K. The determination coefficient (R^2) is usually used to test the reliability of these models. A high R^2 value indicates that the parameters obtained are reliable, and the adsorption process can be described by the model. The R^2 value of the Langmuir isotherm was higher, which meant that it had a higher degree of fitting, and the experimental data could be better explained by this model [45]. The fitting results are shown in Fig. 6. The results show that MB and MG adsorption on regenerated AC is fully consistent with the Langmuir isotherm model, which means that it is a chemical adsorption process based on the affinity of the functional group and binding energy [46,47]. Through the Langmuir isotherm model, the index value of R^2 is close to 1, which verifies that the Langmuir isotherm model is suitable for the experimental data. The application of the Langmuir isothermal model shows that the regenerated AC adsorbed the dye in a single layer, and the enthalpy and activation energy of each molecule were equal. Table 3 shows that the monolayer adsorption capacities of regenerated AC for MB and MG are the largest, which are 265.65 and 366.89 mg/g, respectively. Compared with that of other adsorbents, the adsorption capacity of regenerated AC for MB and MG is better, indicating that the regenerated AC has great adsorption potential for

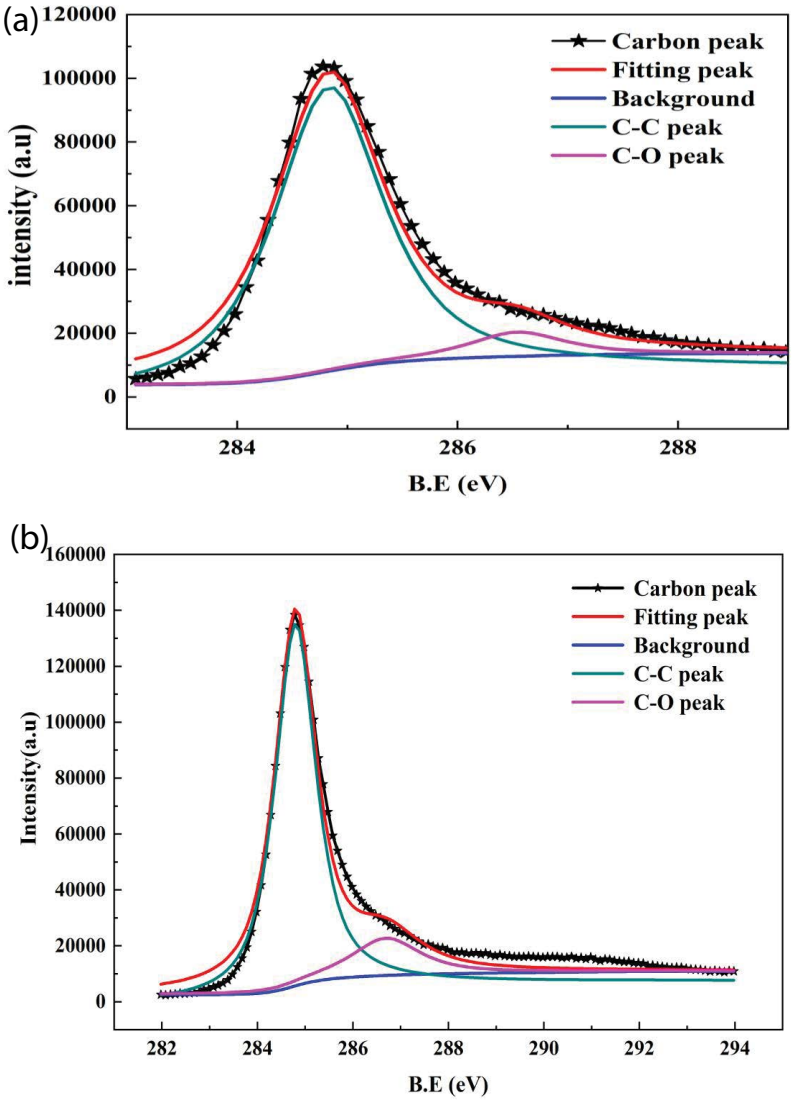

Fig. 4. XPS spectra of (a) waste and regenerated activated carbon.

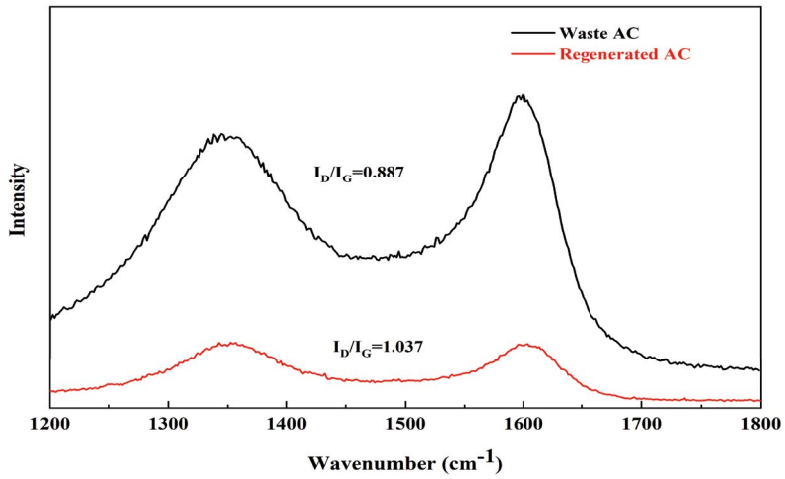

Fig. 5. Raman spectra of regenerated and waste activated carbon.

Table 2
Isotherm parameters for the adsorption of MB and MG onto regenerated AC at 303 K

Isotherms	Parameters	MB	MG
Langmuir	Q_0 (mg/g)	265.65	366.89
	K_L (L/mg)	3.0017	2.4379
	R^2	0.98797	0.99298
Freundlich	$1/n$	0.24799	0.16349
	K_F ((mg/g)(L/mg)$^{1/n}$)	154.21	317.42
	R^2	0.79363	0.88491
Temkin	A (L/g)	187.34	310.95
	B	31.63	29.14
	R^2	0.89843	0.91351

different pollutants. Therefore, it can be concluded that, under the conditions of this study, regenerated AC is useful for adsorbing MB and MG dyes, and the adsorption process is in good agreement with the Langmuir isotherm model.

3.7. Adsorption kinetics analysis

Adsorption kinetics can not only explain the adsorption mechanism of MB and MG on regenerated AC, but also reveal the specific relationship between adsorbate molecules and adsorbents in the equilibrium state [53]. Using MB and MG as adsorbents, the adsorption kinetics of regenerated AC were analyzed. Table 4 lists the related model parameters. The experimental result is in agreement with the pseudo-second-order model, and R^2 approaches 1. Therefore, pseudo-second-order kinetics between the two

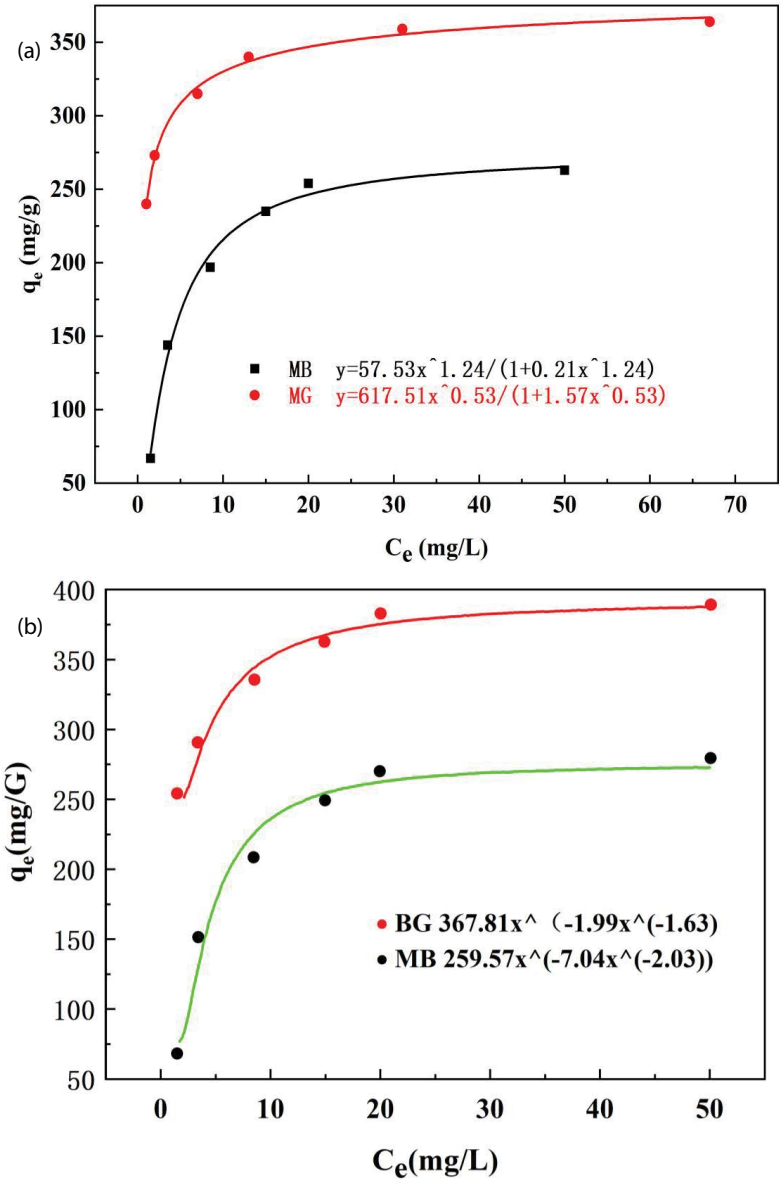

Fig. 6. The adsorption isotherm fitting by (a) Langmuir and (b) Freundlich isotherm.

Table 3
Comparison of maximum capacity using the Langmuir model for MB and MG adsorption onto different activated carbons

Dyes	Adsorbents	Experimental conditions	Adsorption capacity (mg/g)	Reference
MB	Regenerated AC	C_0: 400 mg/L; *m*: 0.2 g; solution: 200 mL; *t*: 120 min	265.65	This work
	Au-AC	C_0: 18 mg/L; *m*: 0.01 g; pH: 7; 1.6 min of ultrasound time	185	[25]
	$CuFe_2O_4$/MWCNTs	C_0: 10–100 mg/L; pH: 5.6; *m*: 0.005g; *T*: 323 K; *t*: 360 min	204	[26]
	Fe_3O_4@CPTES@AG MNPs	C_0:250 mg/L; *m*: 50 mg; *t*: 120 min; pH: 2.5	246.3	[48]
	cSMFB	C_0: 25 mg/L; pH_{MB}: 6.1; *m*: 0.02 g; *T*: 298 K; *t*: 480 min	72	[49]
	Fe-AC	C_0: 400 mL/L; microwave power: 700 W; microwave heating temperature: 700°C; heating time: 25 min	257	[50]
MG	Regenerated AC	C_0: 400 mg/L; *m*: 0.2 g; solution: 200 mL; *t*: 120 min	366.89	This work
	GWAC	C_0:100 mg/L; *m*: 0.02 g; *t*: 180 min; pH: 6.95	154.2	[27]
	BSC	C_0: 80 mg/L; *t*: 100 min; pH: 3	98	[28]
	CSC	C_0: 250 mg/L; solution: 50 mL; *t*: 35 min; pH: 7.4	188.4	[51]
	PPS	C_0: 50 mg/L; *m*: 0.03 g; solution: 20 mL; *t*: 300 min, pH: 4	11.9	[52]

Table 4
Kinetic parameters for the adsorption of MB and MG onto regenerated AC at 303 K

Pseudo-first-order model					
Adsorbate	C_0 (mg/L)	$q_{e,exp}$ (mg/L)	$q_{e,cal}$ (mg/L)	k_1 (1/min)	R^2
MB	250	248.14	113.09	0.0643	0.8436
MG	250	298.12	146.87	0.0457	0.8387
Pseudo-second-order model					
Adsorbate	C_0 (mg/L)	$q_{e,exp}$ (mg/L)	$q_{e,cal}$ (mg/L)	k_2 (g/mg min)	R^2
MB	250	248.14	253.81	0.001743	0.99563
MG	250	298.12	299.40	0.001649	0.99859

models is the best way to explain the adsorption process of MB and MG. The adsorption of MB and MG fitting model is shown in Fig. 7.

Fig. 7a and b show the linear fitting of pseudo-first-order and pseudo-second-order models, respectively. The results showed that the adsorption trend of regenerated AC for MB and MG was basically the same in this study. Table 4 shows the kinetic parameters obtained by fitting the pseudo-first-order model and the pseudo-second-order model. A higher correlation coefficient (R^2) and the improved adsorption amount (q_e) indicated that the model was fitted well, and as shown in Table 4, pseudo-second-order models were suitable to describe the kinetic experimental data, implying that the pseudo-second-order kinetic model was more suitable to describe the kinetics of MB and MG adsorption on regenerated AC. Comparison of the R^2 values for the two models shows that the pseudo-second-order kinetic model fits best because of its highest value (R^2 = 0.99985). This means that the adsorption processes of MB and MG are controlled by chemical processes, which involve electron sharing between the adsorbent and the adsorbent surface [54]. Chemisorption is usually confined to a single layer of molecules on the surface and may be followed by physical adsorption molecules of additional layers [55].

3.8. Adsorption mechanism

Based on the analysis and characterization results of adsorption kinetics and adsorption isotherms, the adsorption of MB and MG by the regenerated AC is a combination of physical adsorption and chemical adsorption, and physical adsorption plays a major role in the adsorption process of dyes. The adsorption mechanism can be explained from two aspects: (1) The pore structure of the regenerated AC provides abundant adsorption sites for the adsorption of MB and MG. (2) MB and MG attract each other through the abundant oxygen-containing functional groups on the surface of the regenerated AC. The adsorption mechanism is shown in Fig. 8.

3.9. Power and energy consumption

The power consumption of waste AC was compared with that of conventional heating and regeneration. To control the temperature at 800°C ± 5°C under microwave heating, the waste AC was heated with a power of 900 W for 10 min to 800°C, and then kept at the required temperature for 40 min. The total heating and holding time is recorded as one cycle, so the total operating time of microwave heating is 50 min, and the power consumption is 0.75 kWh. The same is true for conventional heating. A muffle furnace with a power of 1,200 W is used to heat the waste AC for 30 min to 800°C, and then it is maintained at the required temperature for 120 min. The total heating and holding time is recorded as one cycle, so the total normal running time is 150 min, and the power consumption is 3.00 kWh. In general, microwave heating regeneration of waste AC saves approximately 75% of electricity consumption compared to conventional regeneration.

4. Conclusions

- This study proved that it is feasible to regenerate waste AC containing anthraquinone dye by microwave heating. The best heating temperature was 800°C, and the

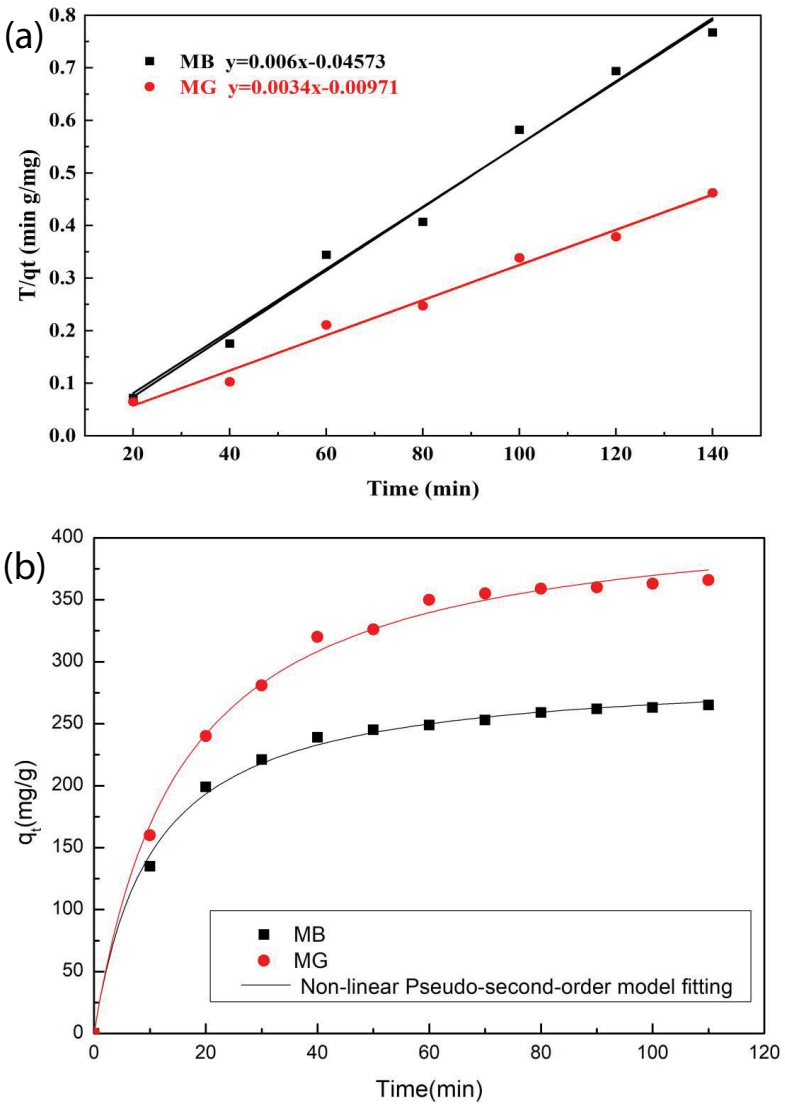

Fig. 7. The adsorption of MB and MG fitting by (a) pseudo-first-order and (b) pseudo-second-order kinetic model.

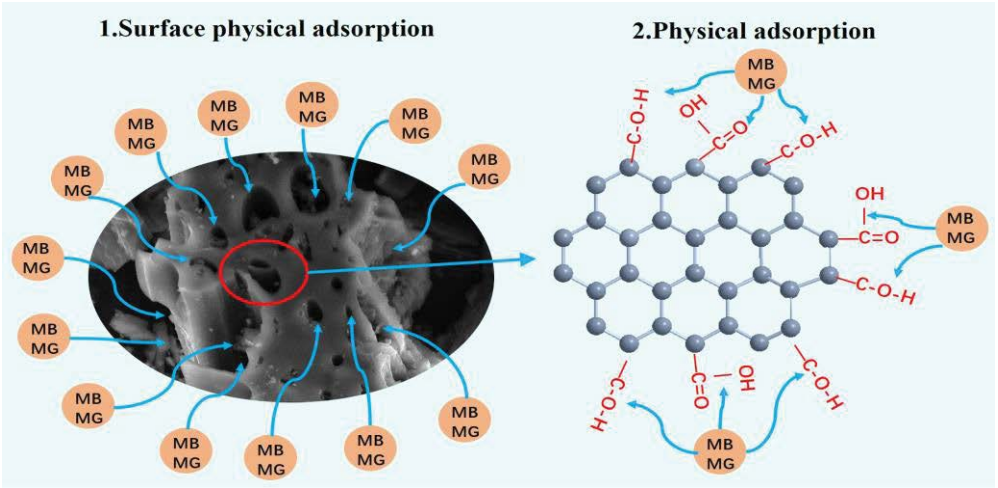

Fig. 8. Adsorption mechanism of MB and MG on regenerated activated carbon.

heating power was 960 W for 40 min. The best experimental conditions showed that 74% of AC was recovered from the result of S_{BET} (634.73 m^2/g).

- The microwave heating regeneration process can remove a large amount of impurities inside the AC, resulting in a larger pore volume and a richer surface chemical structure. The content of CO functional groups is significantly increased, and the surface of the regenerated AC is effectively modified to restore the original active sites and adsorption capacity.
- The adsorption process of MB and MG using regenerated AC is consistent with the Langmuir adsorption isotherm model and the pseudo-second-order kinetic model. The maximum adsorption capacities of regenerated AC for MB and MG are 265.65 and 366.89 mg/g, respectively. This fact confirms that the adsorption of MB and MG by the regenerated AC is a combination of physical adsorption and chemical adsorption.
- In addition, compared with the traditional regeneration method, the power consumption of the microwave heating method is significantly reduced, and the regeneration cost is greatly reduced.

Acknowledgements

This work was supported by the Specialized Research Fund for the National Natural Science Foundation of China (21966019), Yunnan Ten Thousand Talents Plan Industrial Technology Talents Project (2019-1096), Yunnan Ten Thousand Talents Plan Young & Elite Talents Project (2018-73).

References

[1] W. Li, B. Mu, Y. Yang, Feasibility of industrial-scale treatment of dye wastewater via bio-adsorption technology, Bioresour. Technol., 277 (2019) 157–170.
[2] C. Wang, J. Yin, R. Wang, T. Jiao, H. Huang, J. Zhou, L. Zhang, Q. Peng, Facile preparation of self-assembled polydopamine-modified electrospun fibers for highly effective removal of organic dyes, Nanomaterials-Basel, 9 (2019) 116, doi: 10.3390/nano9010116.
[3] M. Ghaedi, A.M. Ghaedi, B. Mirtamizdoust, S. Agarwal, V.K. Gupta, Simple and facile sonochemical synthesis of lead oxide nanoparticles loaded activated carbon and its application for methyl orange removal from aqueous phase, J. Mol. Liq., 213 (2016) 48–57.
[4] H. Wang, Q. Wang, X. Li, Y. Wang, P. Jin, Y. Zheng, J. Huang, Q. Li, Bioelectricity generation from the decolorization of Reactive blue 19 by using microbial fuel cell, J. Environ. Manage., 248 (2019) 109310, doi: 10.1016/j.jenvman.2019.109310.
[5] J. Pierce, Colour in textile effluents-the origins of the problem, J. Soc. Dyers Colour., 110 (1994) 131–133.
[6] Y.-Q. Liu, N. Maulidiany, P. Zeng, S. Heo, Decolourization of azo, anthraquinone and triphenylmethane dyes using aerobic granules: acclimatization and long-term stability, Chemosphere, 263 (2021) 128312, doi: 10.1016/j.chemosphere.2020.128312
[7] M. Svetozarević, N. Šekuljica, Z. Knežević-Jugović, D. Mijin, Agricultural waste as a source of peroxidase for wastewater treatment: insight in kinetics and process parameters optimization for anthraquinone dye removal, Environ. Technol. Innovation, 21 (2021) 101289, doi: 10.1016/j.eti.2020.101289.
[8] A. Khataee, P. Gholami, B. Vahid, S.W. Joo, Heterogeneous sono-Fenton process using pyrite nanorods prepared by non-thermal plasma for degradation of an anthraquinone dye, Ultrason. Sonochem., 2 (2016) 357–370.
[9] E. Routoula, S.V. Patwardhan, Degradation of anthraquinone dyes from effluents: a review focusing on enzymatic dye degradation with industrial potential, Environ. Sci. Technol., 54 (2020) 647–664.
[10] J. Lach, E. Okoniewska, L. Stępniak, A. Ociepa-Kubicka, The influence of modification of activated carbon on adsorption of Ni(II) and Cd(II), Desal. Water. Treat., 52 (2014) 3979–3986.
[11] E.N. Zare, A. Mudhoo, M.A. Khan, M. Otero, Z.M.A. Bundhoo, C. Navarathna, M. Patel, A. Srivastava, C.U. Pittman Jr., T. Mlsna, D. Mohan, P. Makvandi, M. Sillanpää, Water decontamination using bio-based, chemically functionalized, doped, and ionic liquid-enhanced adsorbents: review, Environ. Chem. Lett., 19 (2021) 3075–3114.
[12] M.J. Kampschreur, H. Temmink, R. Kleerebezem, M.S.M. Jetten, M.C.M. Van Loosdrecht, Nitrous oxide emission during wastewater treatment, Water Res., 43 (2009) 4093–4103.
[13] E. Gagliano, M. Sgroi, P.P. Falciglia, F.G.A. Vagliasindi, P. Roccaro, Removal of poly- and perfluoroalkyl substances (PFAS) from water by adsorption: role of PFAS chain length, effect of organic matter and challenges in adsorbent regeneration, Water Res., 171 (2020) 115381, doi: 10.1016/j.watres.2019.115381.
[14] G. Qu, J. Li, Y. Wu, G. Li, D. Li, Regeneration of acid orange 7-exhausted granular activated carbon with dielectric barrier discharge plasma, Chem. Eng. J., 146 (2009) 168–173.
[15] M.A. Yahya, Z. Al-Qodah, C.W.Z. Ngah, Agricultural bio-waste materials as potential sustainable precursors used for activated carbon production: a review, Sustainable Energy Rev., 46 (2015) 218–235.
[16] A. Jain, R. Balasubramanian, M.P. Srinivasan, Hydrothermal conversion of biomass waste to activated carbon with high porosity: a review, Chem. Eng. J., 283 (2016) 789–805.
[17] S.A. Alshareef, M. Otero, H.S. Alanazi, M.R. Siddiqui, M.A. Khana, Z.A. Alothman, Upcycling olive oil cake through wet torrefaction to produce hydrochar for water decontamination, Chem. Eng. Res. Des., 170 (2021) 13–22.
[18] E. Sabio, E. González, J.F. González, C.M. González-García, A. Ramiro, J. Gañan, Thermal regeneration of activated carbon saturated with p-nitrophenol, Carbon, 42 (2004) 2285–2293.
[19] P.P. Falciglia, P. Roccaro, L. Bonanno, G. De Guidi, F.G.A. Vagliasindi, S. Romano, A review on the microwave heating as a sustainable technique for environmental remediation/detoxification applications, Renewable Sustainable Energy Rev., 95 (2018) 147–170.
[20] G. Durán-Jiménez, L.A. Stevens, G.R. Hodgins, J. Uguna, J. Ryan, E.R. Binner, J.P. Robinson, Fast regeneration of activated carbons saturated with textile dyes: textural, thermal and dielectric characterization, Chem. Eng. J., 378 (2019) 121774, doi: 10.1016/j.cej.2019.05.135.
[21] H. Mao, D. Zhou, Z. Hashisho, S. Wang, H. Chen, H. Wang, Constant power and constant temperature microwave regeneration of toluene and acetone loaded on microporous activated carbon from agricultural residue, J. Ind. Eng. Chem., 21 (2015) 516–525.
[22] P.P. Falciglia, E. Gagliano, V. Brancato, G. Malandrino, G. Finocchiaro, A. Catalfo, G. De Guidi, S. Romano, P. Roccaro, F.G.A. Vagliasindi, Microwave based regenerating permeable reactive barriers (MW-PRBs): proof of concept and application for Cs removal, Chemosphere, 251 (2020) 126582, doi: 10.1016/j.chemosphere.2020.126582
[23] R. Malik, D.S. Ramteke, S.R. Wate, Adsorption of Malachite green on groundnut shell waste based powdered activated carbon, Waste Manage., 27 (2007) 1129–1138.
[24] E. Gagliano, P.P. Falciglia, Y. Zaker, T. Karanfil, P. Roccaro, Microwave regeneration of granular activated carbon saturated with PFAS, Water Res., 198 (2021) 117121, doi: 10.1016/j.watres.2021.117121.
[25] M. Roosta, M. Ghaedi, A. Daneshfar, R. Sahraei, A. Asghari, Optimization of the ultrasonic assisted removal of Methylene blue by gold nanoparticles loaded on activated carbon using experimental design methodology, Ultrason. Sonochem., 21 (2014) 242–252.
[26] S.M. Wabaidur, M.A. Khan, M.R. Siddiqui, M. Otero, B.-H. Jeon, Z.A. Alothman, A.A.H. Hakami, Oxygenated functionalities

enriched MWCNTs decorated with silica coated spinel ferrite – a nanocomposite for potentially rapid and efficient de-colorization of aquatic environment, J. Mol. Liq., 317 (2020) 113916, doi: 10.1016/j.molliq.2020.113916.
[27] H. Sayğılı, F. Güzel, Performance of new mesoporous carbon sorbent prepared from grape industrial processing wastes for Malachite green and congo red removal, Chem. Eng. Res. Des., 100 (2015) 27–38.
[28] R. Ahmad, R. Kumar, Adsorptive removal of Congo red dye from aqueous solution using bael shell carbon, Appl. Surf. Sci., 257 (2010) 1628–1633.
[29] G. Lin, L. Zhang, S. Yin, J. Peng, S. Li, F. Xie, Study on the calcination experiments of rare earth carbonates using microwave heating, Green Process. Synth., 4 (2015) 329–336.
[30] I. Langmuir, The constitution and fundamental properties of solids and liquids. Part I. Solids, J. Am. Chem. Soc., 38 (1916) 2221–2295.
[31] K.Y. Foo, B.H. Hameed, Microwave-assisted regeneration of activated carbon, Bioresour. Technol., 119 (2012) 234–240.
[32] S. Cheng, Q. Chen, H. Xia, L. Zhang, J. Peng, G. Lin, X. Liao, X. Jiang, Q. Zhang, Microwave one-pot production of ZnO/Fe_3O_4/activated carbon composite for organic dye removal and the pyrolysis exhaust recycle, J. Cleaner Prod., 188 (2018) 900–910.
[33] N. Solovitch, J. Labille, J. Rose, P. Chaurand, D. Borschneck, M.R. Wiesner, J.Y. Bottero, Concurrent aggregation and deposition of TiO_2 nanoparticles in a sandy porous media, Environ. Sci. Technol., 44 (2010) 4897–4902.
[34] M.A. Beckett, P.N. Horton, M.B. Hursthouse, D.A. Knox, J.L. Timmis, Structural (XRD) and thermal (DSC TGA) and BET analysis of materials derived from non-metal cation pentaborate salts, Dalton Trans., 39 (2010) 3944–3951.
[35] R.K. Agarwal, J.A. Schwarz, Analysis of high pressure adsorption of gases on activated carbon by potential theory, Carbon, 26 (1988) 873–887.
[36] I.A.W. Tan, B.H. Hameed, A.L. Ahmad, Equilibrium and kinetic studies on basic dye adsorption by oil palm fibre activated carbon, Chem. Eng. J., 127 (2007) 111–119.
[37] M. Manes, L.J.E. Hofer, Application of the Polanyi adsorption potential theory to adsorption from solution on activated carbon, J. Phys. Chem., 73 (1969) 584–590.
[38] M.A. Daley, D. Tandon, J. Economy, E.J. Hippo, Elucidating the porous structure of activated carbon fibers using direct and indirect methods, Carbon, 34 (1996) 1191–1200.
[39] P.J.F. Harris, Z. Liu, K. Suenaga, Imaging the atomic structure of activated carbon, J. Phys.: Condens. Matter, 20 (2008) 362–201.
[40] A. Foelske-Schmitz, D. Weingarth, R. Kötz, XPS analysis of activated carbon supported ionic liquids: enhanced purity and reduced charging, Surf. Sci., 605 (2011) 1979–1985.
[41] J. Yu, Z. Meng, C. Chi, X. Gao, K. Qiao, Low temperature pickling regeneration process for remarkable enhancement in Cu(II) adsorptivity over spent activated carbon fiber, Chemosphere, 281 (2021) 130868, doi: 10.1016/j.chemosphere.2021.130868.
[42] R. Liang, Z. Jian, L. Ye, C. Zhang, Preparation and evaluation of cattail fiber-based activated carbon for 2,4-dichlorophenol and 2,4,6-trichlorophenol removal, Chem. Eng. J., 168 (2011) 553–561.
[43] E. Taer, M. Deraman, I.A. Talib, Awitdrus, R. Farma, M.M. Ishak, R. Omar, B.N.M. Dolah, N.H. Basri, M.A.R. Othman, S. Kanwal, Impedance spectroscopic analysis of composite electrode from activated carbon/conductive materials/ruthenium oxide for supercapacitor applications, AIP Conf. Proc., 1656 (2015) 030004, doi: 10.1063/1.4917093.
[44] G. Fu, Z. Li, Measurement and analysis of methane adsorption isotherms on activated carbon, Nat. Gas Ind. B, 24 (2004) 92–94.
[45] E.G. Furuya, H.T. Chang, Y. Miura, K.E. Noll, A fundamental analysis of the isotherm for the adsorption of phenolic compounds on activated carbon, Sep. Purif. Technol., 11 (1997) 69–78.
[46] S. Dawood, T. Kanti Sen, Removal of anionic dye Congo red from aqueous solution by raw pine and acid-treated pine cone powder as adsorbent: equilibrium, thermodynamic, kinetics, mechanism and process design, Water Res., 46 (2012) 1933–1946.
[47] J.S. Cao, J.X. Lin, F. Fang, M.T. Zhang, Z.R. Hu. A new absorbent by modifying walnut shell for the removal of anionic dye: kinetic and thermodynamic studies, Bioresour. Technol., 163 (2014) 199–205.
[48] D.P. Li, Y.R. Zhang, X.X. Zhao, B.X. Zhao, Magnetic nanoparticles coated by aminoguanidine for selective adsorption of acid dyes from aqueous solution, Chem. Eng. J., 232 (2013) 425–433.
[49] M.A. Khan, S.M. Wabaidur, M.R. Siddiqui, A.A. Alqadami, A.H. Khan, Silico-manganese fumes waste encapsulated cryogenic alginate beads for aqueous environment de-colorization, J. Cleaner Prod., 244 (2020) 118867, doi: 10.1016/j.jclepro.2019.118867.
[50] S. Cheng, L. Zhang, H. Xia, J.H. Peng, C. Li, Ultrasound and microwave-assisted preparation of Fe-activated carbon as an effective low-cost adsorbent for dyes wastewater treatment, RSC Adv., 6 (2016) 82, doi: 10.1039/C6RA14082C.
[51] N. Kannan, M. Meenakshisundaram, Adsorption of Congo red on various activated carbons a comparative, study, Water Air Soil Pollut., 138 (2002) 289–305.
[52] S.L. Chan, Y.P. Tan, A.H. Abdullah, S.T. Ong, Equilibrium kinetic and thermodynamic studies of a new potential biosorbent for the removal of Basic Blue 3 and Congo red dyes: pineapple (*Ananas comosus*) plant stem, J. Taiwan Inst. Chem. Eng., 61 (2016) 306–315.
[53] K.Y. Foo, B.H. Hameed, Insights into the modeling of adsorption isotherm systems, Chem. Eng. J., 156 (2010) 2–10.
[54] Z. Liu, Y. Sun, X. Xu, X. Meng, J. Qu, Z. Wang, C. Liu, B. Qu, Preparation, characterization and application of activated carbon from corn cob by KOH activation for removal of Hg(II) from aqueous solution, Bioresour. Technol., 306 (2020) 123154.
[55] E.N. El Qada, S.J. Allen, G.M. Walker, Adsorption of Methylene Blue onto activated carbon produced from steam activated bituminous coal: a study of equilibrium adsorption isotherm, Chem. Eng. J., 124 (2006) 103–110.